8.1) Surface Ionization

Atoms can be ionized, when they are in contact with a hot metal surface (contact ionization).

A prerequisite is, that the ionization energy must be lower than the work function of the material. (E.g. W with an electron affinity of 4.9 eV, is often used.)

If the residence time of the atom at the surface is long enough to reach thermal equilibrium (10^{-5} – 10^{-7} s), then the ionization probability is given by a special version of the Saha equation, the Langmuir-Saha equation.

$$P_i = \frac{n_i}{n_i + n_0} = \left(1 + \frac{g_i}{g_0} \cdot e^{\frac{e(\varphi_i - W)}{kT}}\right)^{-1} \qquad (8.1)$$

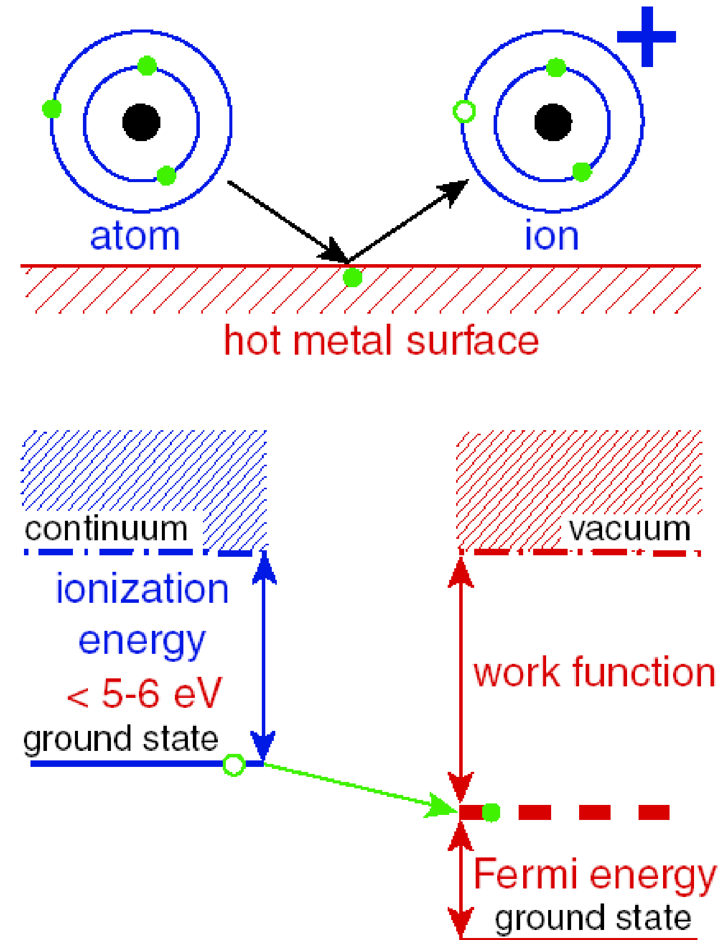

Figure 2.5.1.: Principle of positive surface ionization.

Therein g_i and g_0 are the statistical weights of the ions and neutral particles, φ_i is the ionization potential (ionization energy) of neutral gas atoms and W is the working function of the hot metal surface.

The fraction of ions is small for the most combinations φ_i, W except for alkalines.

Example: K on a 2000 K (0.17 eV) hot Pt-surface

$$\varphi_i = 4.5\,eV, \quad W^{Pt} = 5.65\,eV$$

$$P_i = \left(1 + \frac{1}{2} \cdot e^{\frac{(4.5-5.65)}{0.17}}\right)^{-1} = 0.9994$$

An example for the ionization on Iridium-surfaces is shown on the right. Big advantage of surface ionization is the small energy spread of the ion beams $\Delta W \sim 2kT << 1\ eV$.

One of the important applications:

Production of Cs-ions in sputtering-sources.

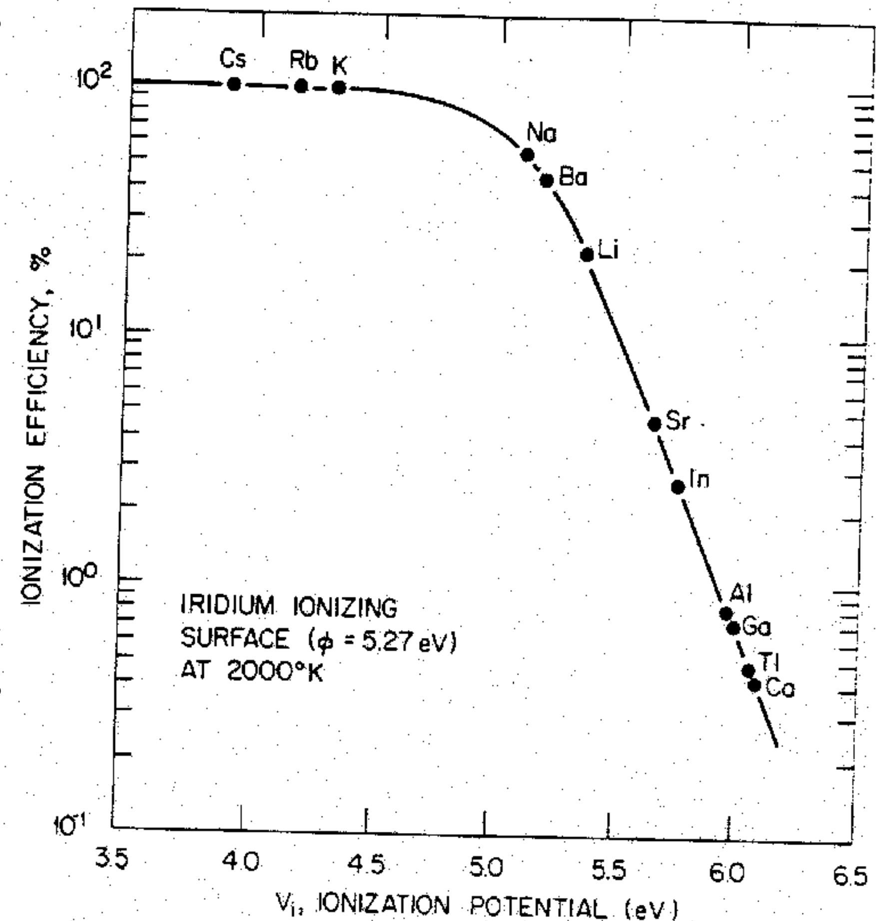

FIG. 45. Surface-ionization efficiencies of the group I, II, and III elements, evaporated from hot iridium metal, calculated from Eq. (3.122).

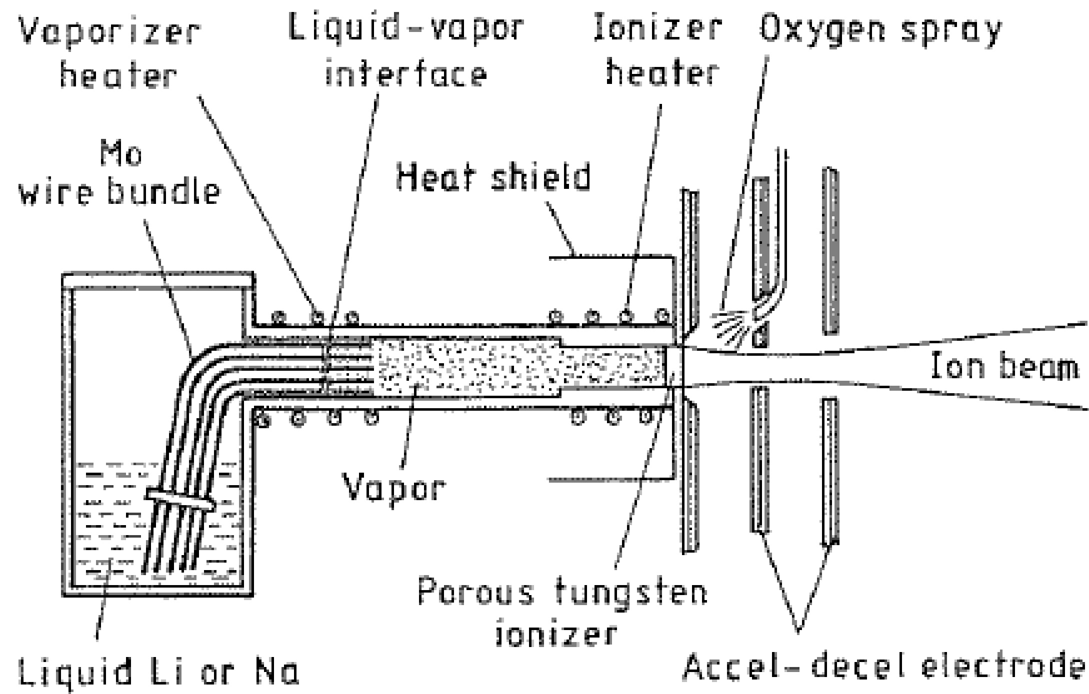

As we can see from Saha-Langmuir-equation, P_i decreases with increasing T, if $\varphi_i - W < 0$.

T must be sufficiently high to evaporate the given element (e.g. Li, Na). On the contrary, the diffusion of surface material must be low enough (< 10% of a mono-layer), to keep the ionization conditions as constant as possible.

In contrast to plasma ion sources, where the extraction optics depend on the shape of the plasma-meniscus, the extraction of surface-sources depends on the shape of the hot surface. Additionally the beam forming is independent of the current density!

Beside Pellets also Zeolites are used (inclusion of the material to be ionized). Sources with 75 mA beam current at 2.5 cm beam diameter are feasible. The reservoir of material within the source determines the lifetime of the source.

Enhancement of efficiency: Hot cavity as ionizer → many contacts of the atoms with the wall → increases P_i

In such a cavity, elements with $\varphi_i \sim 8$ eV can be ionized.

However, only single charged ions are produced!

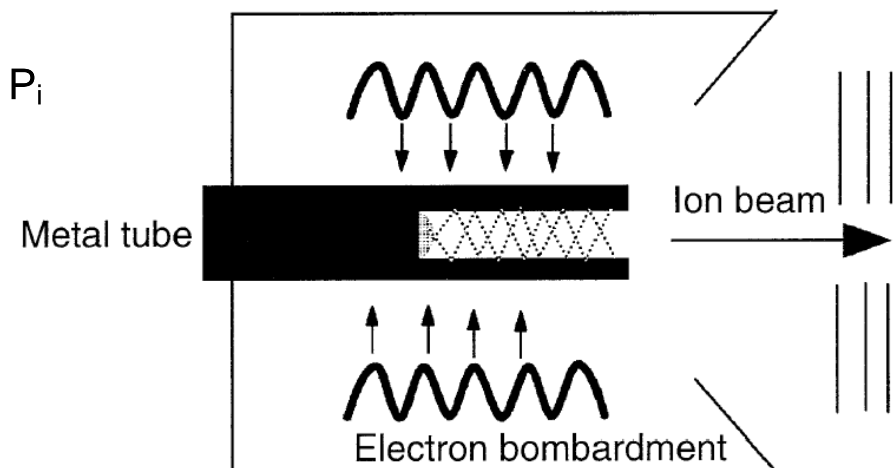

Surface ionization was first investigated by Langmuir in 1923. Later, the advantage of surface covered with Oxygen and Cesium (positive, respectively negative ions) became obvious. For the hot surfaces Tungsten, Iridium or Rhenium are predominantly used.

8.2) Production of negatively charged ions at surfaces

The production of negatively charged ions is predominantly exothermal, in contrary to the production of positively charged ions. Difference to positive ions: at big distances practically no Coulomb-field.

The electron generates its own binding potential, by polarization of the neutral atoms or molecules
Negative ions can be produced by the following processes:

- Volume processes by electron collision
- Charge reversal in metal vapor
- Charge reversal at surfaces

Surface charge reversal:
Uses the low working function of hot metal-surfaces, like in surface ionization or sputter-sources

Example see graphic

Cs atoms are ionized at the hot surface and accelerated towards the target. Therewith, atoms from the target material are sputtered out and negatively charged, especially if the surface of the target is plated with a Cs-layer.

The target can quickly be replaced via a target-wheel (graphic).

Sputter-source:

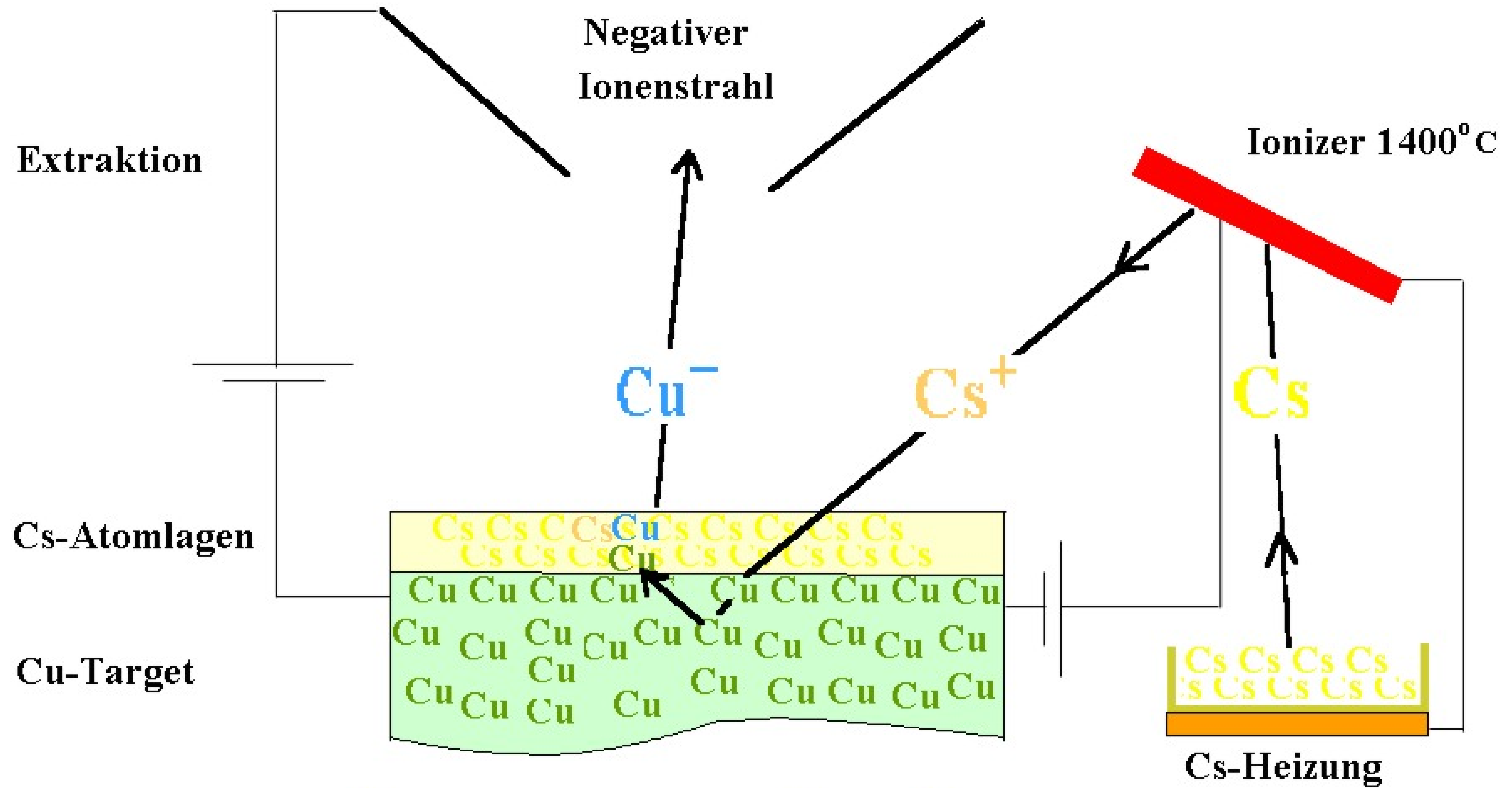

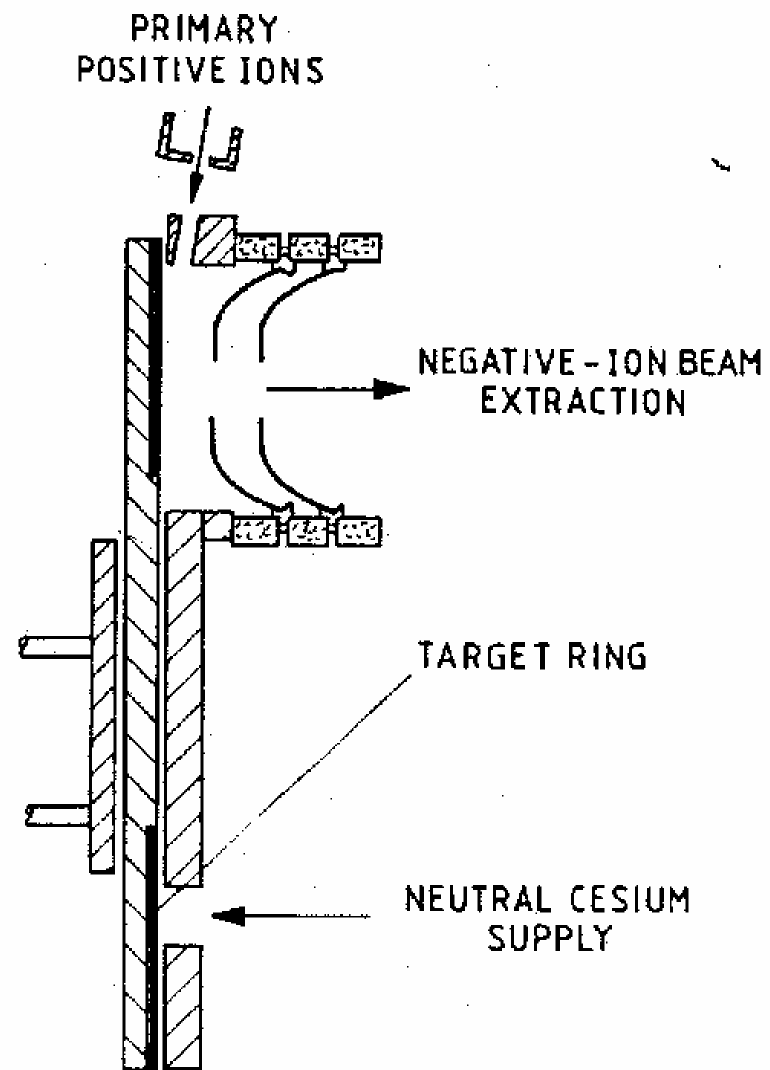

FIGURE 16.1
Sputter type heavy negative-ion source developed by Mueller and Hortig.[23]

<u>Plasma-surface-conversion</u>

The plasma is generated in front of the target and
the target is put onto a negative potential

Ions from the plasma sputter negative ions
out of the bulk material

The production efficiency of negatively charged ions
increases if the atom leaves the metal surface with
velocity v, which is bigger than the thermal velocity.
The electron is transferred during the ejection process.
(see graphic)

An example for the production of negative ions on
a Mg-target is shown in the following graphic on.
the right.

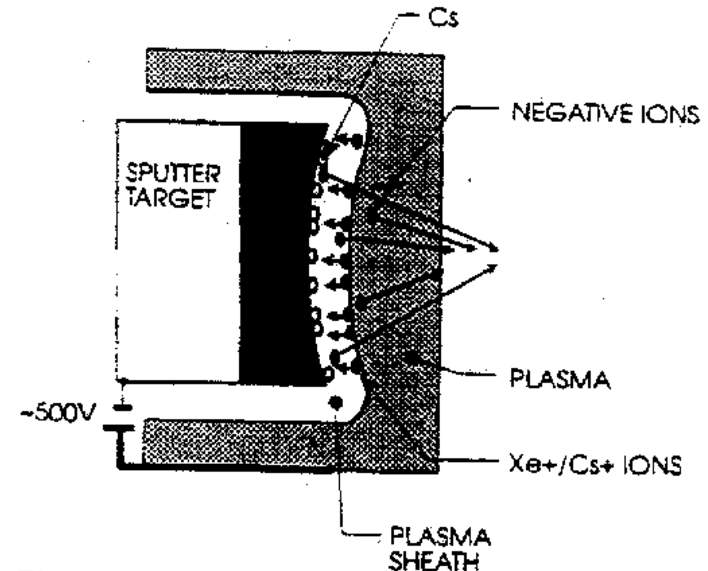

Fig. 23 Schematic of plasme sputter negative ion generation

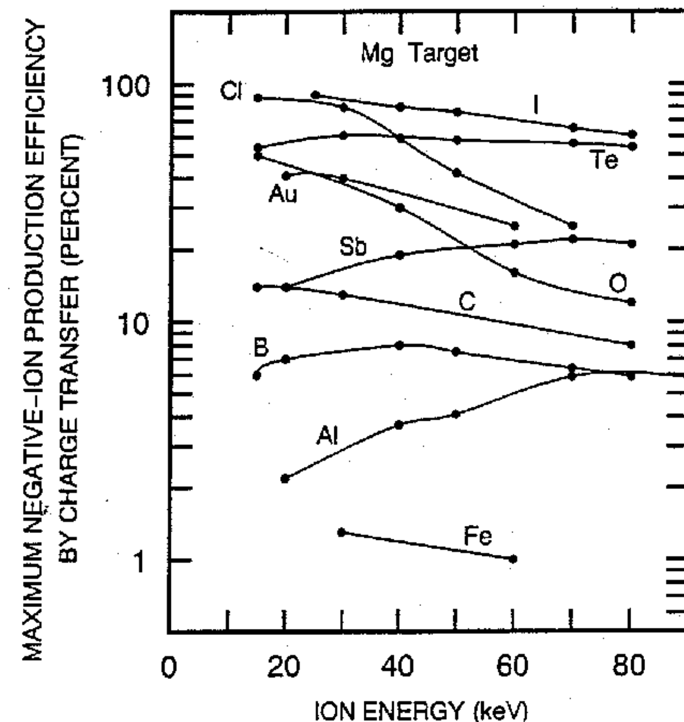

The negative ion current is given by:

$$I^- = I^+ \cdot A \cdot \eta^- \exp(-n_0 L \sigma_d)$$

I^+ = positive ion current, A = Sputter-rate,

η^- = Production efficiency for negative ions at the surface

n_o = Residual gas density, L = free flight path through residual gas

σ_d = cross section for charge reversion

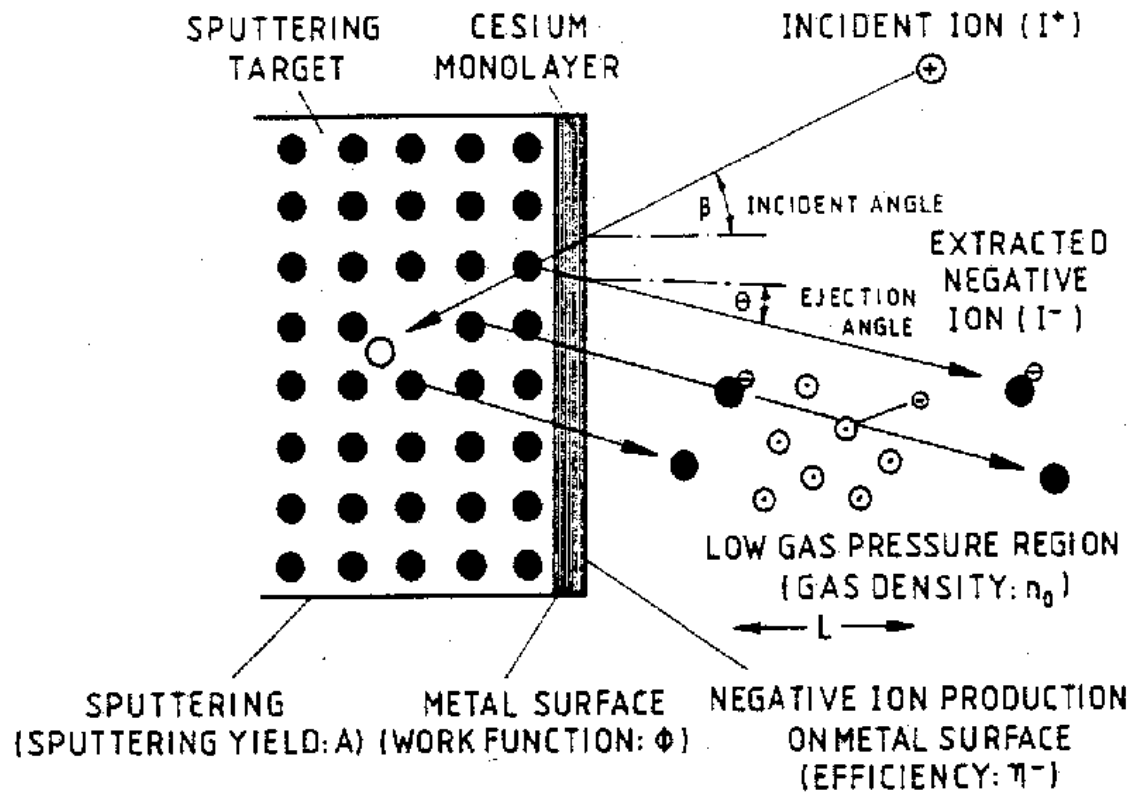

FIGURE 16.6
Illustration of the secondary negative-ion emission process by reflection or sputtering.

8.3) Laser-Plasma ion sources

In contrast to resonant ionization, the plasma within this source is generated via energy deposition.

The laser beam penetrates the material until $f_{Laser} = f_{cutoff}$.

→ local heating of electrons by inverse Bremsstrahlung + excitation of atoms

→ Material is ablated and an expanding plasma-plume develops

If the plasma density has been lowered that the cut-off frequency drops below the laser-frequency, the laser light can re-enter the plasma. Thereby the electrons inside the plasma are accelerated up to 100 keV.

→ highly charged ions, in which $T_e \propto \left(P_{Laser} \cdot \bar{Z}\right)^{2/7}$

(T_e = Electron temperature, P = Laser power, $\bar{Z}$ = average charge state)

The relationship is shown in the following graphic.

high current mode: P ~ 10^9 W/cm^2, E ~ 1 - 50 J, Δt ~ 1 ns

high charge state mode: P > 10^{12} W/cm^2, E ~ 1 - 50 J, Δt ~ 1 - 10 ps

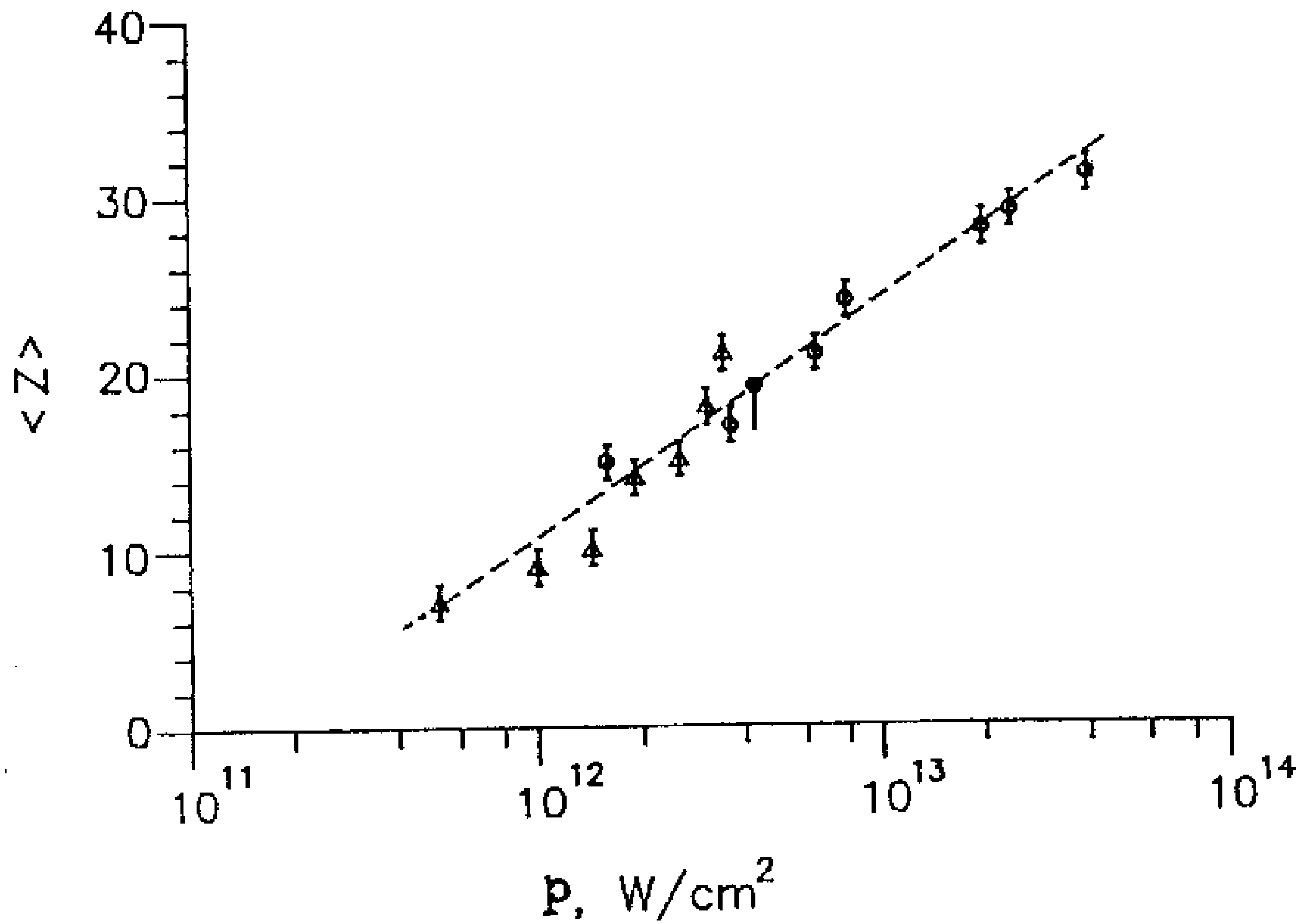

FIGURE 10.2
Dependence of average charge state on laser power density.

Principle of a Laser-Plasma ion source:

The light is focused onto the target by a parabolic mirror (Focus diameter 65 μm)

→ Plasma expands and becomes accelerated

→ Big opening angle, therefore double collimation (before and after expansion chamber)

Disadvantage:

- Big emittance due to plasma-expansion
- big energy-spread (~10%) via the acceleration during expansion

Advantage:

- high charge states
- peak currents of highly charged ions up to 150 mA

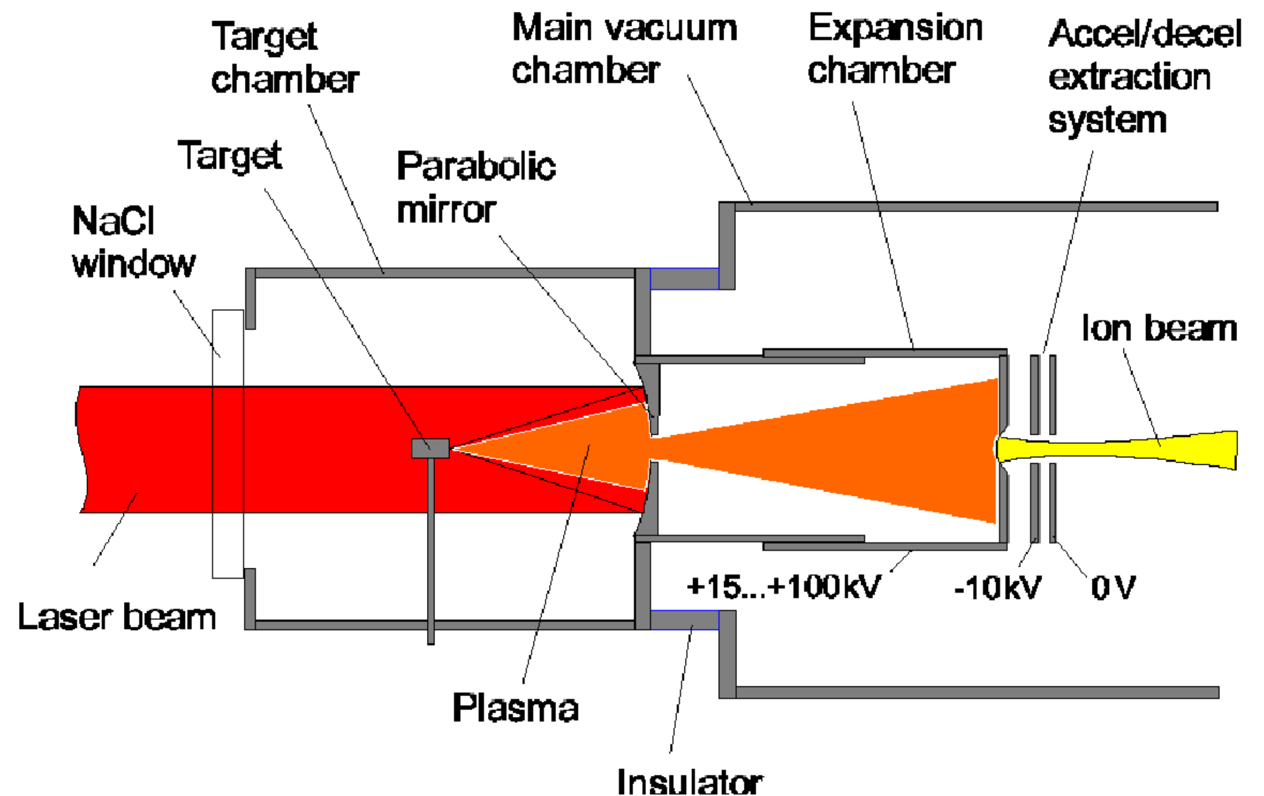

8.4) Electron guns

Until the thirties of the last century, electron beams were only used in highly specialized installations and in accelerators. At the beginning of the forties, electron beams found their application in high-frequency technologies (Klystrons, drift tubes, tetrodes etc.). Electron beams are used in TVs, electron microscopes, for welding- and lithographic devices.

Current: μA to kA

Beam energy: 0.1 to 200 keV

The influence of space charge has the be considered at high beam currents.

Simple diode system:

Deformation of the equipotential lines due to space charge

Space charge adjusts in that way, that the cathode does not see the anode voltage anymore
→ shielding

$$\left.\frac{dU}{dx}\right|_{x=0} = 0$$

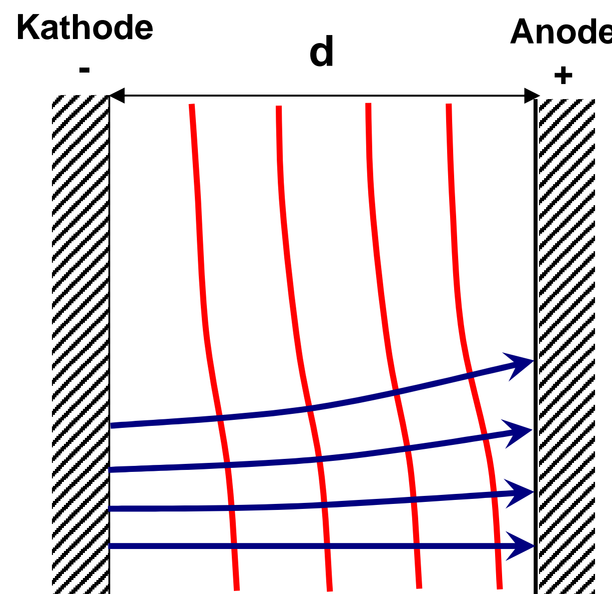

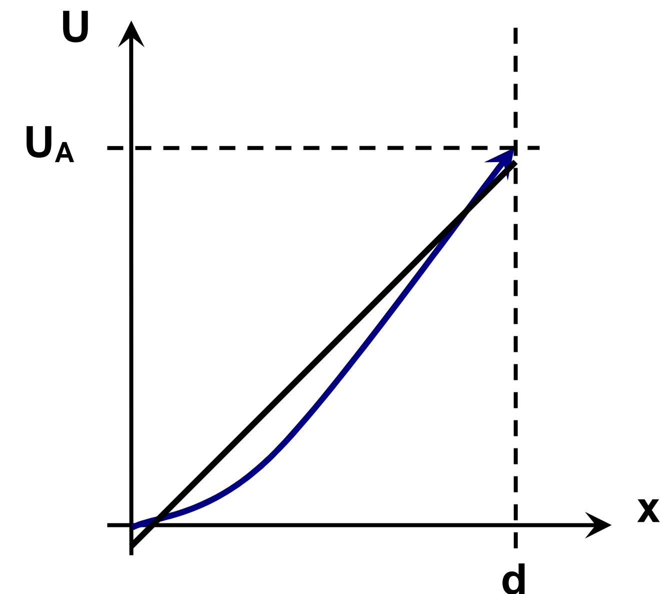

Poisson equation: $$\Delta U = \frac{\partial^2 U}{\partial x^2} = -\frac{\rho}{\varepsilon_0} = \frac{j}{v \cdot \varepsilon_0} = \frac{j}{\varepsilon_0 \sqrt{\frac{2e}{m}}} \frac{1}{\sqrt{U}}$$

Ansatz: $U = A \cdot x^n$ => $U'' = A \cdot n(n-1) \cdot x^{n-2}$

➔ $n = 4/3$ and $A = \left(\frac{9}{4} \frac{j}{\varepsilon_0 \sqrt{\frac{2e}{m}}} \right)^{\frac{2}{3}}$ with boundary condition $U_A = A \cdot d^{4/3}$

therewith one gets the "spase charge limited region" for the emitted current:

$$j = \frac{4}{9} \varepsilon_0 \sqrt{\frac{2e}{m}} \frac{U_A^{3/2}}{d^2}$$

→ **Child-Langmuir-law** (8.2)

with $I = j * F$ F = emitting area

$$I = P \cdot U^{3/2}$$ with P = Perveance (8.3)

In the case of a planar diode system $P = \frac{4}{9} \varepsilon_0 \sqrt{\frac{2e}{m}} \frac{F}{d^2}$

In the case of a cylindrical or spherical symmetry: Solutions from Langmuir and Blodgett

$$I = \frac{16}{9}\pi \cdot \varepsilon_0 \sqrt{\frac{2e}{m}} \frac{U_A^{3/2}}{\alpha^2}$$ → **spherical symmetry** $$I = \frac{8}{9}\pi \cdot \varepsilon_0 \sqrt{\frac{2e}{m}} \frac{U_A^{3/2}}{\beta^2 r}$$ → **cylindrical symmetry**

with $j_c = \frac{4}{9}\varepsilon_0 \sqrt{\frac{2e}{m}} \frac{U_A^{3/2}}{(r_c - r)^2}$ follows $j_{Kugel} = j_c \frac{(r_c - r)^2}{r^2 \alpha^2}$ and $j_{Zylinder} = j_c \frac{(r_c - r)^2}{r^2 \beta^2}$

Thereby r_c is the cathode radius and $\alpha(r)$ und $\beta(r)$ can be represented as a series expansion.

$$\alpha = \gamma - \frac{3}{10}\gamma^2 + \frac{3}{40}\gamma^3 - \frac{63}{4400}\gamma^4 + \frac{13311}{6160000}\gamma^5 - \frac{27 \cdot 10391}{10472 \cdot 10^5}\gamma^6$$ with $\gamma = \ln\left(\frac{r}{r_c}\right)$

Generation of electron beams:

- **thermionic emission**

Richardson-Dushman relation for current density: $j_R = A \cdot b \cdot T^2 \exp\left(-\frac{\phi}{kT}\right) \quad \left[\frac{A}{cm^2}\right]$ (8.4)

Thereby the constant A is $A = \frac{4\pi \cdot m e k^2}{h^3} = 120{,}4 \quad \left[\frac{A}{cm^2 K^2} \right]$

b =material dependent constant
ϕ is the work function, kT the thermal energy of the electrons
j can only be measured if T >> room temperature

Typical response curve for diode:

The domains are

a) Initial current domain

b) Space charge limited regime (Child-Langmuir)

c) Saturation and temperature limited regime

d) is the point were the curve deviates from Child-Langmuir.

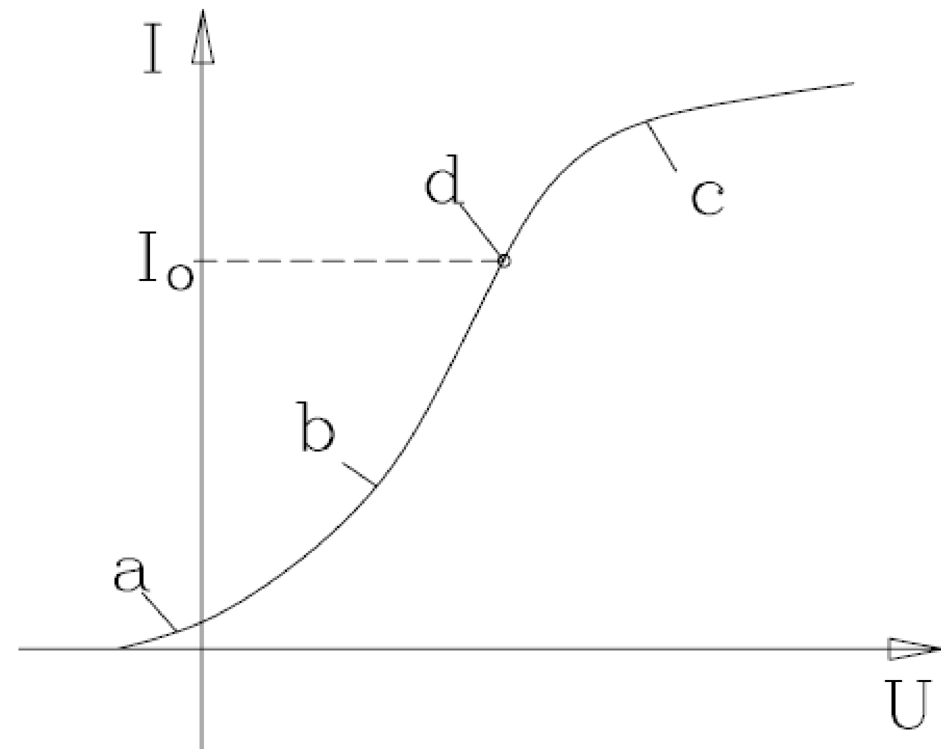

➢ Field emission

E-field of the order of 10^7 V/cm
(eg. at cone points, needle cathodes) thereby the potential at the surface of the solid is lowered insofar that the electrons can tunnel.

-> Fowler-Nordheim equation:

$$j_{FE} = \frac{K_1 U^2}{\phi} \exp\left(-\frac{K_2 \phi}{U}\right) \quad \left[\frac{A}{cm^2}\right] \qquad (8.5)$$

ϕ is the work function, U the applied voltage and K_1 and K_2 constants

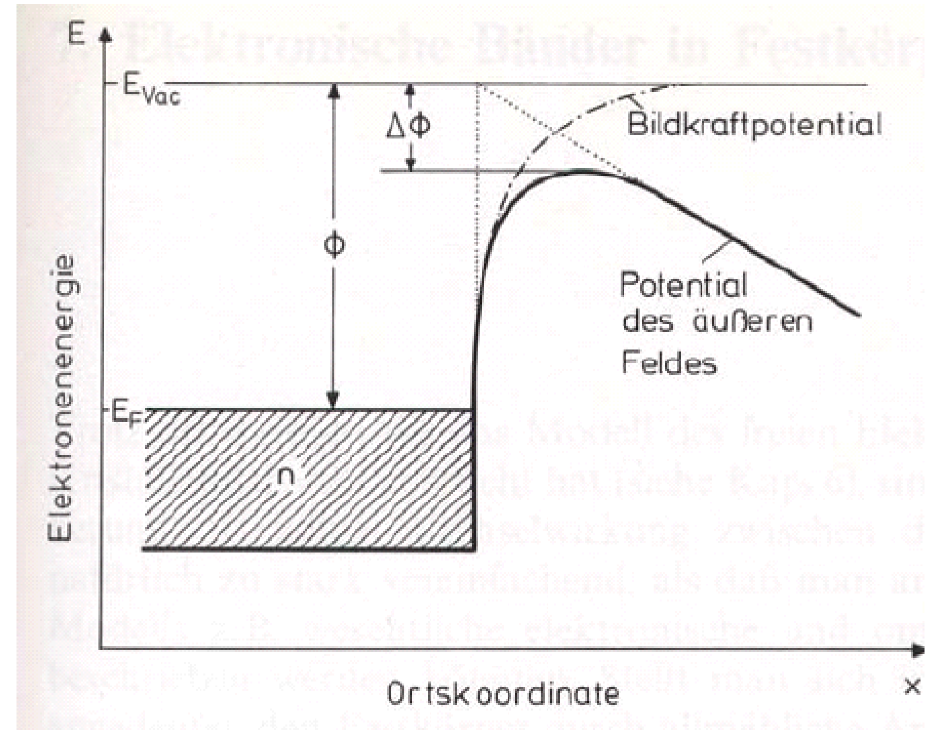

Beam formation in electron guns:

In which way can we shape an electron beam under the influence of space charge?
At the beam boundary there is

$$U = A \cdot x^{4/3} \quad \text{and} \quad \frac{\partial U}{\partial y} = -E_y = 0 .$$

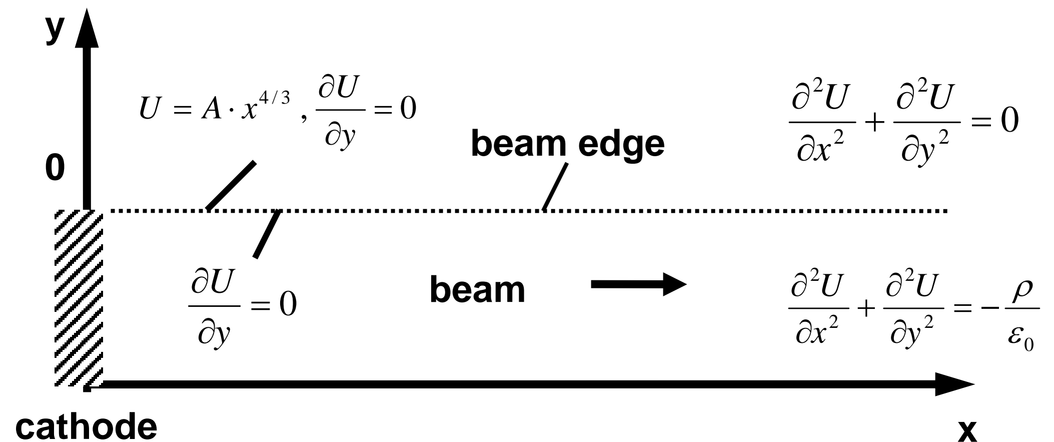

This is a Cauchy-boundary-condition, at which the field strength is given!

In this case it holds: $U\big|_{y=0} = f(x)\,,\ \left.\frac{\partial U}{\partial y}\right|_{y=0} = 0$

The potential outside the x-axis ($y \neq 0$) is the analytical continuation of the function f(x) in the complex plain: $U(x,y) = \mathrm{Re}(f(z)) = \mathrm{Re}(f(x+iy))$

Taylor expansion: $f(x+iy) = f(x) + iy \cdot f'(x) + \frac{(iy)^2}{2!} f''(x) + \cdots$

➔ $$U(x,y) = f(x) - \frac{y^2}{2} f''(x) + \cdots \quad , \quad U(x,0) = f(x) \quad , \quad \left.\frac{\partial U}{\partial y}\right|_{y=0} = -y \cdot f''(x)\big|_{y=0} = 0$$

Thus, for the beam boundary it is

$$U(x,y) = \mathrm{Re}(A \cdot (x+iy)^{4/3}) = Ar^{4/3}\,\mathrm{Re}(\exp(\tfrac{4}{3} i\varphi))$$

==> $U(x,y) = A \cdot r^{4/3} \cos(\tfrac{4}{3}\varphi) = A\left(x^2 + y^2\right)^{2/3} \cos\left(\tfrac{4}{3}\arctan(\tfrac{y}{x})\right)$

The cathode potential $U_c = 0$ one can find with $\cos\left(\frac{4}{3}\varphi\right) = 0$.

Hence, the angle is:

$$\varphi = \frac{3\pi}{8}, \frac{9\pi}{8}$$ or

$$\varphi = 67.5°, 202.5°$$

The cathode boundary needs an angle of 67.5° towards the cathode normal to compensate for the divergence of the space charge dominated beam.

⇒ Boundary cathode with Pierce type boundary

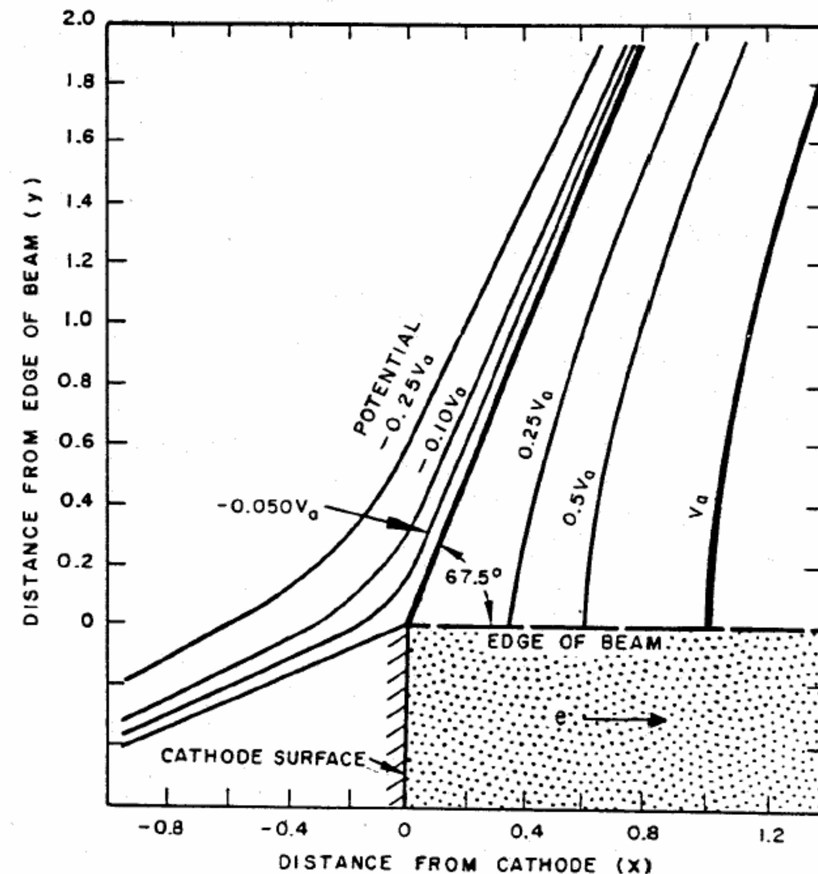

FIG. 4. Plot of the equipotential lines external to a planar space-charge-limited electron beam, as determined from Eq. (7). The heavy lines show the shape of the focus electrode and anode electrode.

Beam formation of a Pierce-type electron gun calculated for an anode voltage of 1000 V.
1 mm is equal to 4 meshes!

8.66E-3 A, crossover at R= 25.0, Z=204 mesh unitsmax current density on axis=204

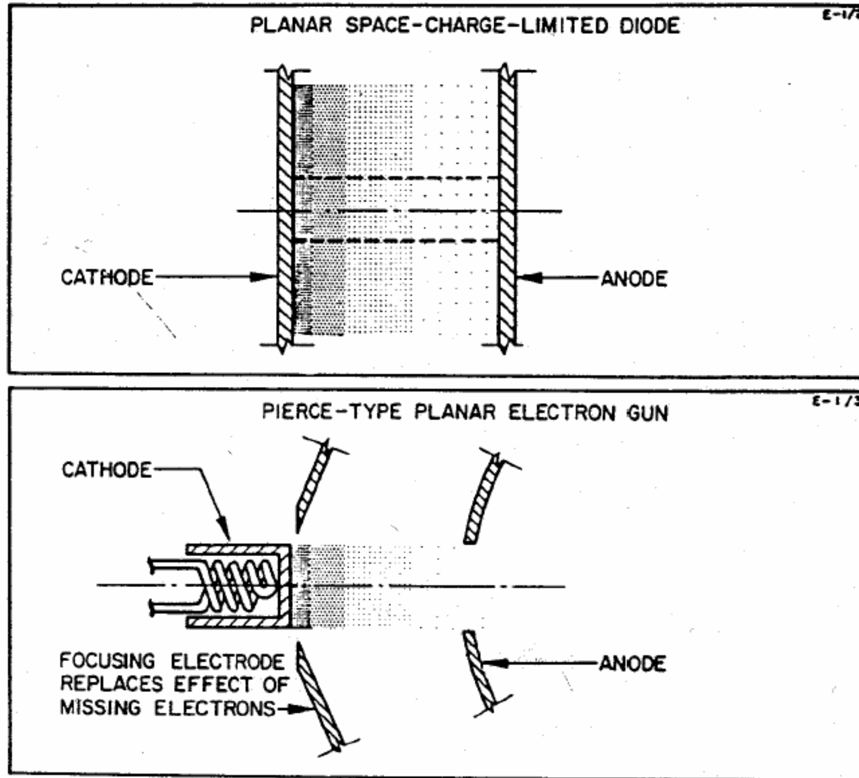

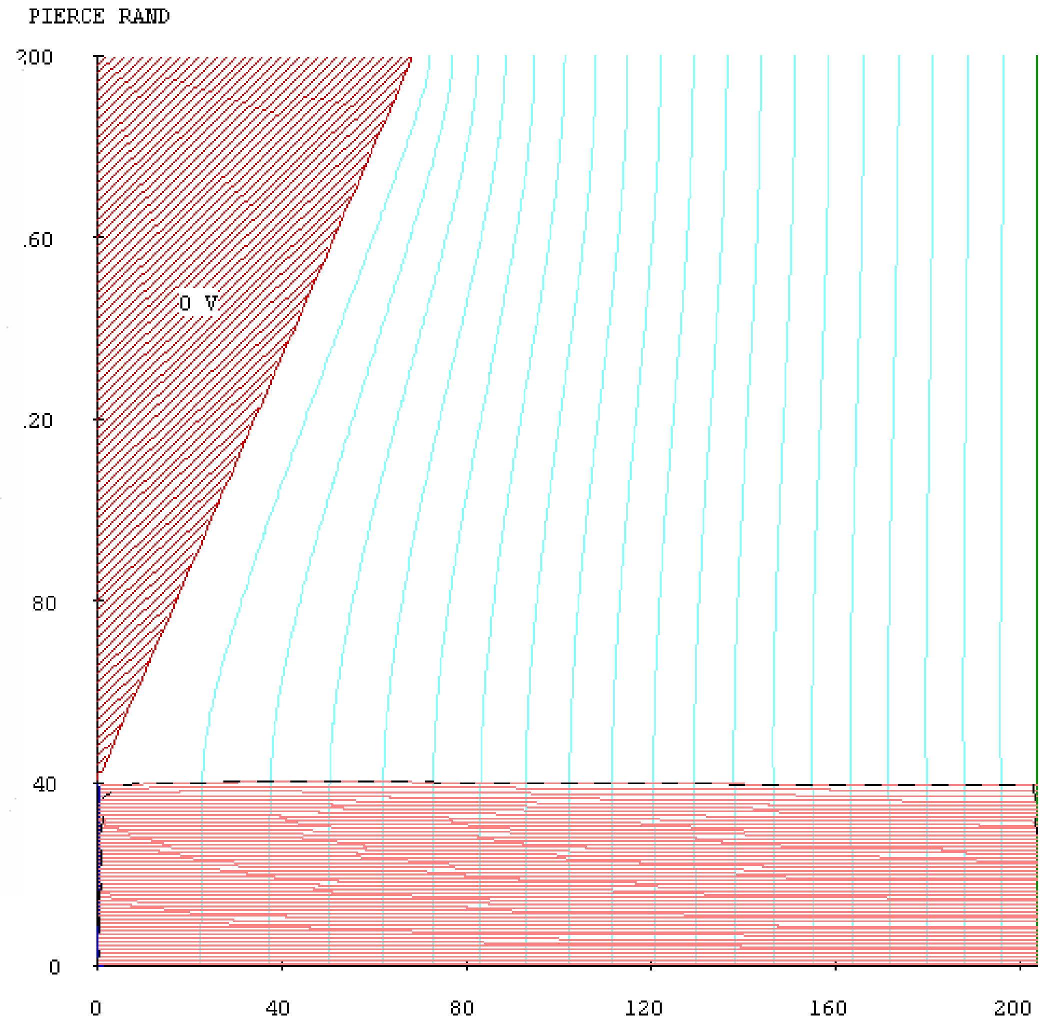

IGUN-7.008(C)R.Becker - RUN 05/27/07*001, file=PIERCE.EIN

Perveance of such a gun:
$P=2.9*10^{-7}$ A/$V^{3/2}$, current I = 9 mA

One can also form the equipotential lines with a Wehnelt cylinder.

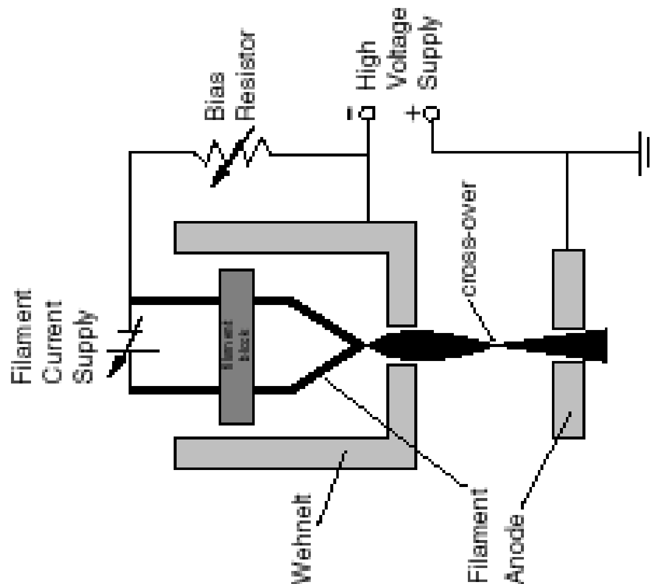

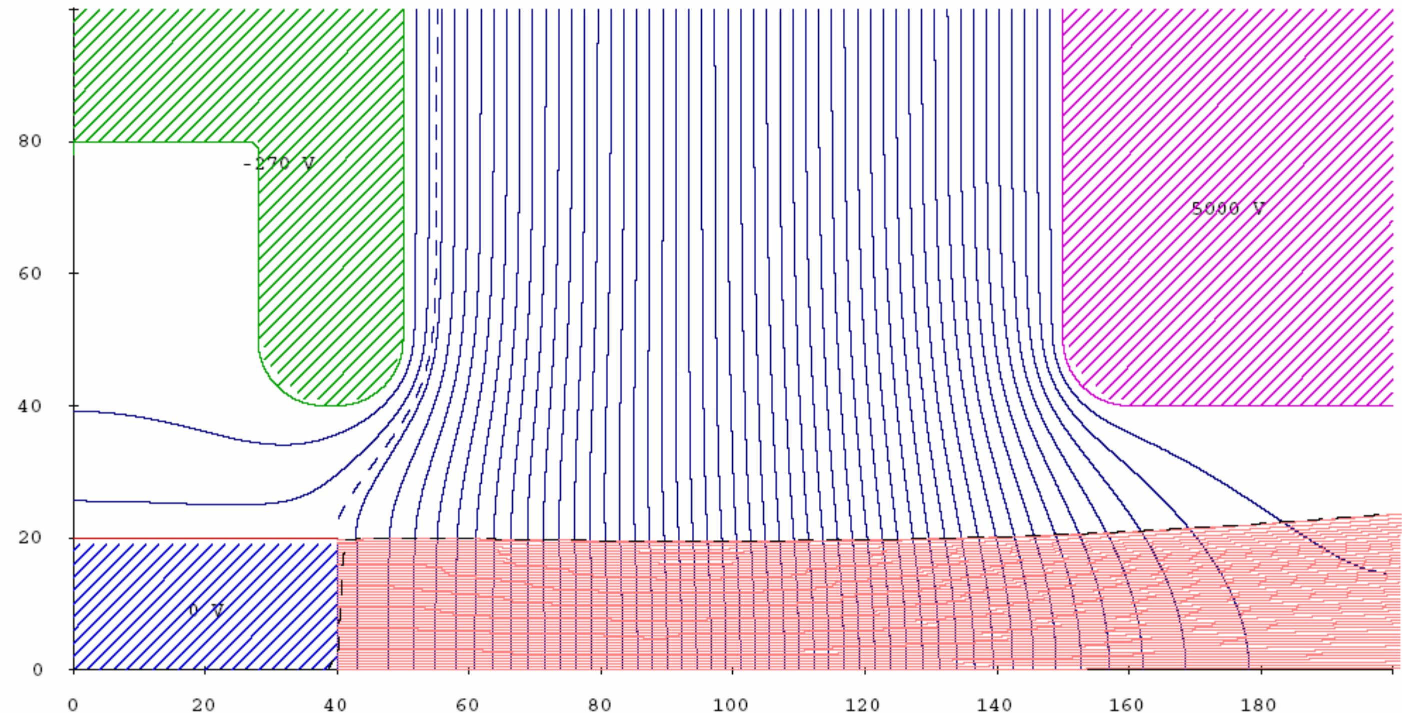

Therewith the potential at the Wehnelt-electrode is adjusted in that way, that the equipotential line, which represent the cathode potential, touches the cathode edge under the Pierce-angle. Wehnelt cylinders are used in electron microscopes and TVs.